

# Microscopic origin of bipolar resistive switching of nanoscale titanium oxide thin films

Hu Young Jeong and Jeong Yong Lee <sup>a)</sup>

*Department of Materials Science and Engineering, KAIST, Daejeon 305-701, Korea*

Min-Ki Ryu and Sung-Yool Choi <sup>b)</sup>

*Electronics and Telecommunications Research Institute (ETRI), Daejeon, 305-700, Korea*

We report a direct observation of the microscopic origin of the bipolar resistive switching behavior in nanoscale titanium oxide films. Through a high-resolution transmission electron microscopy and an analytical TEM technique using energy-filtering transmission electron microscopy, we revealed that oxygen vacancies were formed at the top interface by an oxidation-reduction reaction between the titanium oxide layer and the top Al electrode. We found that the drift of oxygen vacancies during the on/off switching induced the bipolar resistive switching in the titanium oxide thin films.

---

<sup>a)</sup> Electronic mail: [j.y.lee@kaist.ac.kr](mailto:j.y.lee@kaist.ac.kr)

<sup>b)</sup> Electronic mail: [sychoi@etri.re.kr](mailto:sychoi@etri.re.kr)

The bistable switching phenomenon, reversible switching between a high resistance state and a low resistance state, have been discovered for various binary oxide films such as NiO,<sup>1</sup> Nb<sub>2</sub>O<sub>5</sub>,<sup>2</sup> Al<sub>2</sub>O<sub>3</sub>,<sup>3</sup> SiO<sub>2</sub>,<sup>4</sup> and TiO<sub>2</sub>.<sup>5</sup> Since the recent publication by Baek et al.<sup>6</sup> in 2004, resistive random access memory (RRAM) using simple binary transition metal oxides such as NiO and TiO<sub>2</sub> has attracted extensive attention as a high-potential next-generation nonvolatile memory (NVM) due to its simple process, simple device structure, and high CMOS compatibility.<sup>7-9</sup> In the fundamental point of view, the electrical properties of nanoscale binary oxide thin films provides gives deeper understanding of the recently rediscovered memristors, the missing component of the basic circuits elements. Hewlett-Packard (HP) group<sup>10,11</sup> suggested that the motion of dopants or impurities, such as oxygen vacancies acting as mobile +2 charged dopants, was able to produce remarkable changes in the device resistance (memristic behavior), especially in TiO<sub>x</sub> devices. To verify the above models, it is crucial to identify the origin and movement of oxygen vacancies in the actual device structures. However, researchers have not fully shown direct evidence of oxygen vacancies yet.

In this letter, we report on the presence and movement of oxygen vacancies formed by a redox reaction at the Al/TiO<sub>x</sub> top interface through a high-resolution transmission electron microscopy (HRTEM) and an analytical TEM technique using energy-filtering transmission electron microscopy (EFTEM), which provide straightforward information on the microstructure and elemental distribution in the nanoscale films.

To fabricate the Al/TiO<sub>x</sub>/Al memory device, a TiO<sub>x</sub> oxide film with a thickness of ~15 nm was deposited on an Al/SiO<sub>2</sub>/Si substrate by the PEALD (ASM Genitech MP-1000) method at a substrate temperature of 180 °C. The aluminum bottom and top electrodes were deposited by thermal evaporation method, forming the cross-bar type structures using a metal shadow mask with a line width of 60 μm. The cross-sectional images and chemical

analysis of Al/TiO<sub>x</sub>/Al samples were examined by HRTEM and electron energy loss spectroscopy (EELS). A 300 kV JEOL JEM 3010 with a 0.17 nm point resolution and a high-voltage electron microscope JEOL ARM-1300 operating at 1250 keV equipped with energy-filtering TEM were used. For the preparation of a thin cross-sectional TEM sample in two different resistance states (On/Off), we used a conventional TEM preparation method instead of the focused ion beam technique because the latter has more chance to damage the samples. It was also possible to prepare conventional cross-sectional samples since the line width of shadow mask was deliberately increased to 500 μm. The electrical property (I-V curve) was measured using a Keithley 4200 Semiconductor Characterization System in a Dc sweep mode.

Figure 1 shows the typical J-V characteristic of an Al/TiO<sub>x</sub>/Al memory cell with the device structure as depicted in the inset at room temperature under the DC voltage sweep. The J-V curve exhibits a clear hysteretic and asymmetric behavior. Bistable resistance switching between a high-resistance state (HRS) and a low-resistance state (LRS) was induced by the opposite polarity of the applied voltage. The resistance changes from HRS to LRS in the negative bias region, and from LRS to HRS in the positive bias region. It was reported by Yu et al.<sup>12</sup> that this bipolar resistive switching (BRS) was associated with the charge trap sites in the top domain of the Ti oxide thin layer. The right bottom inset of Fig. 1 shows a cross-sectional bright-field (BF) TEM image of the Al/TiO<sub>x</sub>/Al heterostructure with three distinctive layers (the Al bottom electrode, the Ti oxide thin layer, and the Al top electrode). It reveals that the highly uniform Ti oxide layer has been deposited due to an excellent roughness of an Al bottom electrode and the self-limited surface reactions of the atomic layer deposition method.

To clearly characterize the interface regions, we performed the HRTEM measurements of the sequential samples during the fabrication processes. Figure 2 is a series of cross-

sectional HRTEM images of stacked Al/TiO<sub>x</sub>/Al layers which were observed sequentially before and after depositing the titanium oxide thin layer. Note that the very thin native aluminum oxide with a 2~3 nm thickness was already been present before the ALD process, as shown in Figure 2a. Figure 2b displays the HRTEM image of the surface of the Al bottom electrode annealed at 180°C, that is, the same temperature as in the ALD process chamber. It can be inferred that the native aluminum oxide expands to the 3~4 nm thickness due to a thermal annealing effect during the specimen loading process in the ALD main chamber. The uniform titanium oxide film was deposited on the native aluminum oxide with a 400 cycle ALD process. In Figure 2c, it can be seen that the as-deposited titanium oxide layer with a dark contrast clearly has an amorphous phase with a thickness of ~15 nm. After the aluminum thermal evaporation process, the top interface was formed on the titanium oxide thin film, showing the amorphous phase with a light contrast, as shown in Figure 2d. In addition, it is remarkable that the top domain of the titanium oxide layer also has a light contrast, as compared with Figure 2c. (See the red dotted lines in Figures 2c and 2d). It is noted that the composition of the upper Ti oxide layer has been drastically changed due to the reaction with the top aluminum metal layer during the deposition process. Generally, aluminum is well known as one of the most readily oxidizable metals. Therefore, aluminum atoms easily attract oxygen atoms from the titanium oxide layer and react with them, forming a new interfacial Al oxide layer.<sup>13</sup> This oxidation-reduction process induces the oxygen vacancies in the region of titanium oxide; however, it seems doubtful that the nearest upper region displayed as a light contrast in Figure 2d really has oxygen vacancies.

The chemical change of an amorphous titanium oxide thin layer sandwiched between two aluminum electrode, in the off and on states, was characterized in detail using EELS analysis. Energy-filtered EELS elemental mapping with a spatial resolution of less

than 1nm using ultra-high voltage TEM is a very powerful tool for identifying the elemental distribution in an area of only a few nanometers. EELS elemental mapping was obtained using the ‘three window technique’.<sup>14</sup> Figures 3 shows EELS energy-filtered oxygen maps and corresponding intensity profiles of the regions marked with white rectangular areas, visualizing the distribution of oxygen in the off and the on states specimens, respectively. Mapping images were recorded around the O-K (532 eV) edges in the electron energy loss spectrum using a 20 eV energy selecting slit. From these elemental mapping images, the average gray profiles along a line perpendicular to the interfaces with a width of 20nm were obtained from the starting point (a) to the ending point (b). One remarkable finding from Figure 3a and 3c is the oxygen deficiency existing in the middle region of titanium oxides. Many researchers have believed that oxygen vacancies at the metal-oxide interface perform the critical function of bistable resistive switching. However, from the above the EELS result, it is found that the oxygen concentration at the interface very close to aluminum top electrode is much higher than that of the inner part, as displayed in red in the color scale. This can be explained via an oxygen diffusion process. When the interaction between aluminum and titanium oxide occurred at the top interface, the insufficient oxygen ions was added continuously from the below bulk domain. As a result, the bulk region underneath the top interface became more oxygen deficient than the top interface. Thus, it is suggested that these oxygen vacancies present on the top bulk domain become a huge factor in the charge trapping sites and cause bulk space-charge-limited-conduction (SCLC). In particular, the EELS oxygen mapping image of the on state, shown in Figure 3b and 3d, interestingly shows that oxygen ions driven into the top interface region are equally distributed through the titanium oxide inner part. It can be understood that oxygen ions are able to move in the  $\text{TiO}_x$  amorphous active layer by strong external electric field. Unlike the top interface, the bottom interface does not show a

considerable change. This is associated with the native aluminum oxide layer having immobile oxygen ions. Due to this native oxide layer, the transition from the off state to on is not observed when positive bias applied to the top Al electrode. This asymmetric interface characteristic induces the bipolar switching phenomena in Al/TiO<sub>x</sub>/Al devices.

Based on the HRTEM images and energy-filtered EELS images mentioned above, the mechanisms of oxygen vacancy formation in the titanium oxide thin layer sandwiched between two Al electrodes and the positively charged oxygen vacancies drift by external electrical bias can be described schematically, as shown in Figure 4. A native aluminum oxide layer with 2~3 nm thickness was present on the surface of the bottom Al electrode after the thermal evaporation process on a SiO<sub>2</sub>/Si substrate. When the top Al electrode deposition started in the thermal evaporation chamber, aluminum atoms attached to the surface of the titanium oxide and formed Al metal layers, where they gathered oxygen ions present in the top TiO<sub>x</sub> layer, and resulted in the formation of the top interface amorphous layer owing to strong oxygen affinity and oxygen ions in the middle region diffused into the Al/TiO<sub>x</sub> top interface by an oxygen concentration gradient. Therefore, the oxygen deficient domain, shown in Figure 4b, was established at the bulk TiO<sub>x</sub> region. This state corresponds to the off state in Al/TiO<sub>x</sub>/Al memory devices. While sufficient negative bias is applied to the top Al electrode, the positively charged oxygen vacancies piled up at the bulk TiO<sub>x</sub> region drift to the top interface, causing the device to switch to the on state.

In summary, we have demonstrated that the drift of oxygen vacancies in the applied bias was attributed to the microscopic origin of the bistable resistivity switching. From the sequential cross-sectional HRTEM images and energy-filtered TEM elemental mapping analysis, it is justified that oxygen vacancies formed at inner region of bulk TiO<sub>x</sub> film can drift as external bias exceeds the threshold field. These analyses give the direct evidence of

the memristic behaviors and the deeper understanding of the bipolar resistive switching mechanisms of binary oxides.

## **Acknowledgments**

This work was supported by the Next-generation Non-volatile Memory Program of the Ministry of Knowledge Economy, Korea. The authors sincerely thank Youn-Joong Kim at Korea Basic Science Institute (KBSI) for the use of the high-voltage electron microscope and the technical staffs of the Process Development Team at ETRI for their support with the PEALD facility.

## **References**

- <sup>1</sup>J. F. Gibbons and W. E. Beadle, *Solid-St. Electron.* **7**, 785 (1964).
- <sup>2</sup>W. R. Hiatt and T. W. Hickmott, *Appl. Phys. Lett.* **6**, 106 (1965).
- <sup>3</sup>F. Argall, *Electron. Lett.* **2**, 282 (1966).
- <sup>4</sup>R. W. Brander, D. R. Lamb, and P. C. Rundle, *Brit. J. Appl. Phys.* **18**, 23 (1967).
- <sup>5</sup>F. Argall, *Solid-St. Electron.* **11**, 535 (1968).
- <sup>6</sup>I. G. Baek, M. S. Lee, S. Seo, M. J. Lee, D. H. Seo, D.-S. Suh, J. C. Park, S. O. Park, H. S. Kim, I. K. Yoo, U-In Chung, and J. T. Moon, *Dig. – Int. Electron Devices Meet.* **2004**, 587.
- <sup>7</sup>I. G. Baek, D. C. Kim, M. J. Lee, H.-J. Kim, E. K. Yim, M. S. Lee, J. E. Lee, S. E. Ahn, S. Seo, J. H. Lee, J. C. Park, Y. K. Cha, S. O. Park, H. S. Kim, I. K. Yoo, U-In Chung, J. T. Moon, and B. I. Ryu, *Dig. – Int. Electron Devices Meet.* **2005**, 750.
- <sup>8</sup>M.-J. Lee, S. Seo, D.-C. Kim, S.-E. Ahn, D. H. Seo, I.-K. Yoo, I. G. Baek, D.-S. Kim, I.-S. Byun, S.-H. Kim, I.-R. Hwang, J.-S. Kim, S.-H. Jeon, and B. H. Park, *Adv. Mater.* **19**, 73

(2007).

<sup>9</sup>M.-J. Lee, Y. Park, D.-S. Suh, E.-H. Lee, S. Seo, D.-C. Kim, R. Jung, B.-S. Kang, S.-E. Ahn, C. B. Lee, D. H. Seo, Y.-K. Cha, I.-K. Yoo, J.-S. Kim, and B. H. Park, *Adv. Mater.* **19**, 3919 (2007).

<sup>10</sup>J. J. Yang, M. D. Pickett, X. Li, D. A. A. Ohlberg, D. R. Stewart, and R. S. Williams, *Nature Nanotech.* **3**, 429 (2008).

<sup>11</sup>D. B. Strukov, G. S. Snider, D. R. Stewart, and R. S. Williams, *Nature* **453**, 80 (2008).

<sup>12</sup>L.-E. Yu, S. Kim, M.-K. Ryu, S.-Y. Choi, and Y.-K. Choi, *IEEE Electron Device Lett.* **29**, 331 (2008).

<sup>13</sup>U. Diebold, *Surf. Sci. Rep.* **48**, 53 (2003).

<sup>14</sup>L. Reimer, *Energy-Filtering Transmission Electron Microscopy*, Springer Verlag, Berlin, 387 (1995).



## Figure Captions

FIG. 1. Current density-voltage (J-V) characteristics of a typical Al/TiO<sub>x</sub>/Al memory device. Cross-sectional BF TEM image of Al/TiO<sub>x</sub>/Al sandwiched structure deposited on a SiO<sub>2</sub> (3000 Å)/Si substrate is shown in the right bottom inset.

FIG. 2. (Color online) A series of the cross-sectional HRTEM images of Al/TiO<sub>x</sub>/Al heterostructures observed step by step: a) Image showing the existence of native aluminum oxide at the aluminum metal surface. b) Image indicating the broadening of native aluminum oxide by the thermal annealing. c) Image obtained after depositing amorphous titanium oxide thin film by a 400 cycle PEALD process. d) Completed cell image acquired by thermal evaporation deposition of the aluminum top electrode.

FIG. 3. (Color online) Energy filtered-TEM elemental (oxygen) maps of two different samples (the off and on resistance state): a) EELS based oxygen elemental map of as-grown Al/TiO<sub>x</sub>/Al structure, corresponding to the off state. b) Oxygen elemental map of the sample applied negative set bias (-3 V) on the top Al electrode, corresponding to the on state. c) and d) are the corresponding average intensity profiles obtained from the white rectangular areas.

FIG. 4. (Color online) Schematics of proposed models for a) and b) the formation of oxygen vacancies working as the microscopic origin of bipolar resistive switching based on the oxidation/reduction near the interface between the Al top electrode and Ti oxide thin film, and c) the oxygen vacancy drift by the negative bias applied to the Al top electrode.

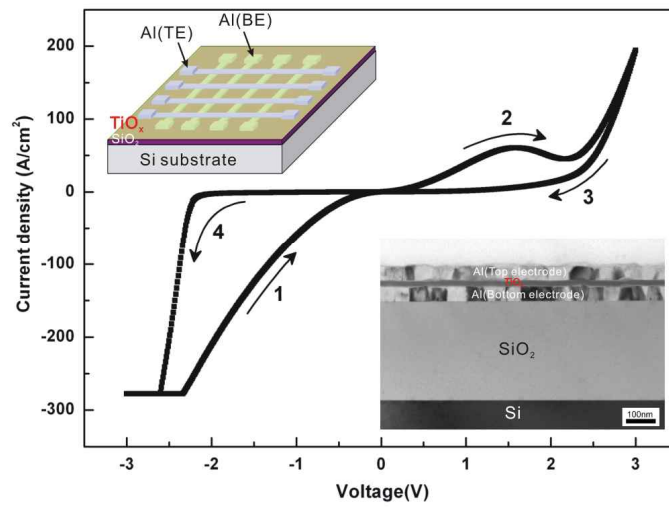


Figure 1 (H. Y. Jeong et al.)

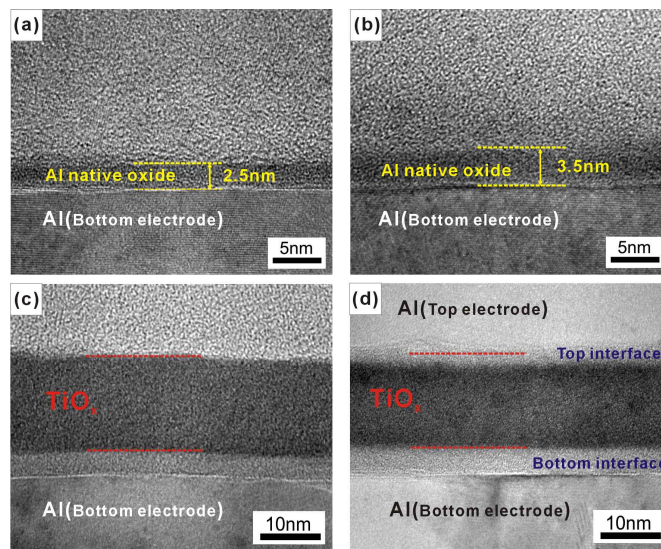


Figure 2 (H. Y. Jeong et al.)

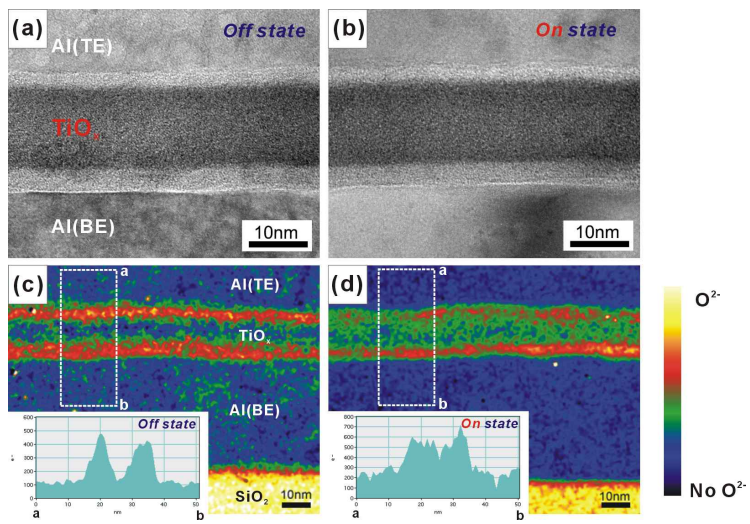


Figure 3 (H. Y. Jeong et al.)

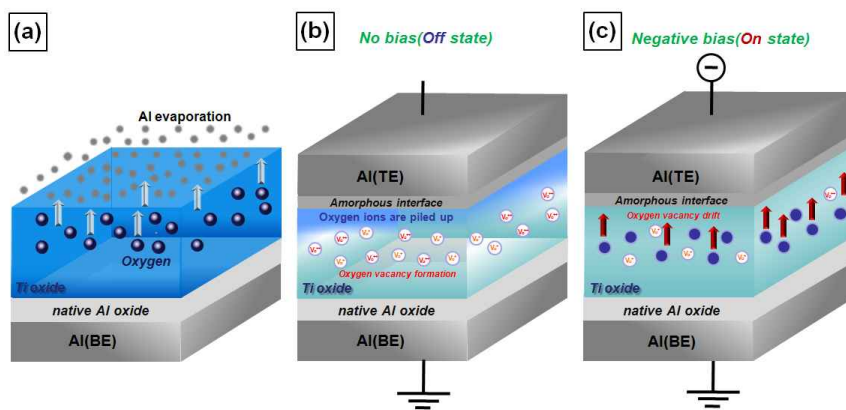


Figure 4 (H. Y. Jeong et al.)